COO-3122-6

Conf-730815--5

PRE-EQUILIBRIUM PROCESSES

by
J. M. Miller

Columbia University

September, 1973

Paper presented at IUPAP, Munich, 1973

DISCLAIMER

PRE-EQUILIBRIUM PROCESSES*

J.M. Miller, Dept. of Chemistry, Columbia University, New York, New York 10027, U.S.A.

I. INTRODUCTION

The treatment of nuclear reactions involving complex nuclei immediately encounters all of the misery of the many-body problem. As usual, the solution is either to turn it essentially into a two-body problem soluble by quadrature, or to treat the many bodies by quasi-equilibrium theory. Direct-reaction theory includes the former approximation while the latter is encompassed by compound-nucleus reactions. The great successes and pervasive usefulness of these two extreme approximations are very fortunate and very well-known. It is, perhaps, less well-known that there is a large body of experimental data that appears to deviate systematically from the predictions of either of these two approximations. A good example is afforded by some of the results obtained by Bertrand and Peele[1] in their comprehensive study of reactions induced by protons up to 62-MeV with targets ranging from carbon to bismuth. The energy spectra of protons emitted in the (p, xp) reaction with 61.7-MeV protons on targets of ^{54}Fe, ^{56}Fe, and ^{60}Ni are shown in Figure 1. There are three readily discernible energy regions in these spectra; the region up to about 10 MeV which exhibits the shape expected for compound nucleus reactions as well as relative magnitudes that reflect the effects of binding energies and level densities on the amount of available phase space; the region above about 53 MeV where the characteristic peaks corresponding to the excitation of particular low-lying states in the target by direct processes are seen; and, finally, the large region from 10 to 50 MeV characterized by its lack of features and indifference to target. It is this featureless and indifferent part of the spectrum that will occupy our attention here and is now called "pre-compound" decay.

Perhaps the earliest recognition of the phenomena entailed was by Serber[2] in his study of nuclear reactions induced in complex nuclei by protons with energies of a few-hundred MeV. The essence

of his idea was that there is a series of direct processes in the form of successive nucleon-nucleon collisions within the nucleus that are generated by the incident high-energy nucleon which results in the direct emission of some of the nucleons that participate in the consequent collisional cascade. It is these emissions that are considered by neither conventional compound-nucleus nor the usual direct-reaction theory. A schematic representation of the general idea is illustrated in Figure 2. The level of sophistication of computers that can calculate the results of this model has increased markedly since 1947; the level of thinking about the problem has not.

The direct simulation of these intranuclear cascades was first carried out by Goldberger[3] in two dimensions by the Monte Carlo technique and subsequently first computerized and considered in three dimensions by Metropolis et al.[4] There have been subsequent refinements of this class of calculation by Bertini, Barashenkov and co-workers, and a Brookhaven-Columbia collaboration which are described, along with references, and compared in reference 5.

Other formalisms for investigating essentially the same physical model, successive two-body collisions, have been developed more recently. These include what has become known as the exciton model put forth by Griffin[6] and elaborated in a series of papers by Blann and co-workers[7-13] as well as the group at Milan.[14-18] Another approach to the same problem by a Columbia-Brookhaven[19,20] collaboration entails the solution of a suitably modified Boltzmann equation.

It is my intention in this paper to summarize briefly and to intercompare these three formalisms with particular emphasis on recent advances, refinements, and to offer criticisms. The Monte Carlo simulation of the intra-nuclear cascade generated by incident nucleons will be given somewhat greater attention partly because it has received less attention in the past, partly because it more explicitly exposes the physical model that is assumed without becoming lost in the complex book-keeping of particles and configurations that is required by all of the formalisms, and mainly because it contains all of the geometrical information inherent in the reactions and thus yields angular as well as energy distribu-

tions of the pre-compound emission.

Some general remarks about the problem are offered in Section II; the Monte Carlo simulation, Boltzmann equation, and exciton model are briefly described and discussed in Sections III, IV, and V, respectively; the models are compared with each other, and the present situation and prospects are sketched in Section VI. Readers who are familiar with these models will be well advised to go directly to Section VI. It might be well at this point to anticipate Section VI and complete the introduction by a warning that is often seen by travelers through underdeveloped areas:

CAUTION

WORK IN PROGRESS

PROCEED AT YOUR OWN RISK

II. GENERAL REMARKS

The present treatments of pre-compound decay are all, in essence, classical as opposed to quantum muchanical and thus they ignore any coherent effects as well as uncertainty-principle constraints. In some of the calculations, proper account is taken of the Pauli exclusion principle, but even that is not always true. Niether the problems inherent in this approach nor its possible justification will be discussed here. Instead, the classical approach will be accepted and the discussion will revolve around investigation of its consequences.

For purposes of discussion, the classical approach to the emission of particles in a nuclear reaction may, in a time-dependent manner, be written as:

$$\frac{d^2\sigma_\nu}{d\Omega\, d\varepsilon} = \sigma_r \sum_Q \int_0^{E_{max}} dE \int_0^{\infty} dt\; W(E,Q,t)\; \lambda(\nu,\varepsilon,\theta \mid E,Q,t) \qquad (1)$$

In this expression, σ_r is the reaction cross section, W(E,Q,t) is the probability per unit energy that the reacting system (a concept that will be defined more carefully later) is characterized by an excitation energy E and in a state Q at a time t, and $\lambda(\nu, \varepsilon, \theta \mid E, Q, t)$ is the probability per unit time that the reacting system when in such a state emits a particle of type ν at an angle θ and with a kinetic energy ε. It should be immediately stated that the variables Q and E should be redundant: a characterization of a state Q should immediately give the corresponding excitation energy, E. However, both for clarity of exposition and because Q in one of the formalims to be considered, the ~~ecitation~~ excited model, does not

determine $\underline{E}$, this redundancy will be accepted. What in general is meant by $\underline{Q}$ is a set of quantum numbers that defines the state of the system, including its mass and atomic number, within the context of the model that is used and might, for example, be the occupation number of the neutron and proton states in the reacting system.

It is to be noted that at all times

$$\sum_{Q} \int W(E,Q,t)\, dE = 1 \qquad (2)$$

At very short times, the main contribution W(E,Q,t) comes from those states that look like "doorway" states; at relatively long times, the W(E,Q,t) are governed by the random distribution of the excitation energy among the available states (the compound-nucleus situation); and, of course, at very long times, the W(E,Q,t) correspond to the relative yields of residual nuclei in their respective ground states. The first task, then, is to estimate W(E,Q,t) at intermediate times before the compound-nucleus situation obtains.

The central feature of pre-compound emission, is that at these intermediate times the excitation energy is focused on a rather few degrees of freedom and the direction of the incident particle is not yet forgotten thereby leading to the emission of more and higher-energy particles in the forward direction. The evolution in time of the various W(E,Q,t) depends on two processes: 1) internal interactions which lead to new and more complex states, and 2) the emission of particles. In all of the models to be considered here, the internal interactions are taken to be two-body collisions between nucleons, while the estimate of particle-emission rates comes from either time-reversal considerations or considerations of the detailed trajectories of excited particles. It is the competition between these two processes that is decisive in determining both the magnitude and the shape of pre-compound spectra.

As will be discussed in somewhat more detail in the separate sections on each of the three formalisms, the calculations have all shown a tendency to underestimate the magnitude of the pre-compound decay. This situation is somewhat remedied when it is explicitly recognized that an important part of pre-compound emission occurs when the excitation is concentrated in the outer diffuse region of the nucleus. Clear experimental evidence for this is seen in the recent work of Bertrand and Peele, as exhibited in Figure 3, where it is seen that the cross-section for pre-compound decay varies as the cube root of mass number of the target as expected for peripheral collision. This effect appears naturally in the Monte Carlo simulation but has to be grafted on to both of the other formalisms.

III. MONTE CARLO SIMULATION

A. General Description of Model: The Monte Carlo simulation of the evolution of a nuclear reaction solves equation 1 by sampling many intra-nuclear cascades of the type illustrated in Figure 2 where appropriately random choices are made of impact parameters, collision partners and sites, and energy and momentum transfer in the successive nucleon-nucleon collisions.[4,5,21-24] The parameters that characterize the nucleon-nucleon collisions are taken to be the same as those in free space at the same relative velocity except that scatterings that would leave one of the collision partners in an already occupied state are rejected. The target nucleus is taken to be a Fermi gas with a step-function density-distribution chosen to approximate the usual Fermi distribution. The many other details as well as the differences in their treatments by the three laboratories that are active in the field are delineated in the references given above.

In terms of equation 1, then, this approach essentially characterizes the state of the nucleus at any time by means of the momenta and coordinates of each of the nucleons that have become involved in the cascade. The emission of particles within this model simply corresponds to the crossing of the sharp boundary defined by the outermost step in the step-function potential that corresponds to the step-function density-distribution. The calculation of the Brookhaven-Columbia group actually follows the evolution of each intra-nuclear cascade in time; the other two follow successively the fastest moving particle in each cascade from collision to collision.

B. Edge Effects: As stated earlier this method of calculation naturally brings in the importance of the diffuse edge of the nucleus for non-compound processes. This is illustrated in Figure 3 where the open circles are values that have been calculated by Bertini. The dependence of the cross section for pre-compound emission of protons and the mass number of the target is reproduced rather well although, as was also stated earlier, the calculation appears to underestimate the amount of pre-compound decay.

C. The Effect of Refraction: The attempt to reproduce the radial variation of the nuclear density and thus the concomitant radial variation of the nuclear potential energy raises the question of the effect of the refraction of the cascade particles as they move through the nucleus. This question has been investigated by the Brookhaven-Columbia group[22] who found, as expected, that the inclusion of the refraction of the cascade-particle trajectories diminished significantly the already-too-small calculated amount of pre-compound emission. This result is expected because of two consequences of the refraction: 1) particles are refracted toward the central higher-density region of the nucleus with a consequent decrease in the mean-free-path and probability for escape, and 2) particles with enough energy to escape from the nucleus may be reflected back into the interior while on their way out.

D. Velocity-Dependent Potential and Nucleon Correlations: There are two other effects, though, which should be added to the calculation if the physical implications of the model are to be more completely explored:

1) the well-known velocity dependence of the nuclear potential, and
2) the granular structure of nuclear matter as compared to the continuous structure inherent in the manner in which the choice of collision sites is made in these calculations.

Introduction of a reasonable velocity-dependent potential had little effect on the results of these calculations;[23] explicit recognition of the granular structure of the nucleus by imposing a minimum distance between successive nucleon collisions resulted in a significant increase in the number of pre-compound particles that are emitted.[24] This latter result is not surprising since, after all, the most probable distance between collisions in the continuous approximation is zero. In figure 4, taken from Bertrand and Peele,[1] there is presented a comparison between Monte Carlo calculations from the Brookhaven-Columbia groups which do (the dotted histogram), and from Bertini which do not (the solid histogram), include the effects of refraction, velocity-dependent potential, and minimum allowable distance between collisions. Compari-

sons should be restricted to energies above about 15 MeV since lower energies include a compound-nucleus contribution which is included in the Bertini calculation but not in the other. Further, the Brookhaven-Columbia calculation was included only for the 15- and 45- degree hisotgrams. It is immediately seen from the 45- degree data that inclusion of the effects mentioned above significantly lowers the cross section for pre-compound emission. As will be seen shortly, the effect is very much larger for heavier nuclei.

E. Angular Distributions: There are a few other points that should be made from Figure 4 in which the experimental results are also presented. Firstly, it should be noted from the 15- degree results that the calculated quasi-elastic peak extending from about 50 - 60 MeV which is in serious conflict with the experimental results is removed when the effects of refraction are included. This quasi-elastic peak arises in the calculation from a single scattering of the incident particle in the diffuse edge of the nucleus; refraction diminishes this class of event dramatically.

Secondly, it should be noted that agreement between experiment and calculation is quite poor at small angles but gets much better at 45 and 75 degrees. Thus, because of the effect of solid angle, comparisons between calculated and experimental angle-integrated energy spectra can give a misleading impression of the overall validity of the various approximate models for pre-compound emission. This distortion can be seen even more dramatically with heavier target nuclei as is illustrated in Figure 5, again taken from reference 1. At 15 degrees it is clear that the calculated shape and magnitude bear little resemblance to the experimental results; by 45 degrees, the agreement is reasonable. This is in sharp contrast to comparison with the angle-integrated spectra illustrated in Figure 6 taken from Blann[25] in which the agreement between the solid histogram (Bertini's calculation is designated as ORNL) and the experimental results is rather good. Figure 6, incidentally, also shows graphically how the inclusion of refractive effects in the cascade calculation (the dotted histogram labeled BNL) seriously diminishes the amount of pre-compound decay.

Thirdly, while it is not a large cross section, it is seen in Figure 5 that the cascade calculation without refraction seriously underestimates the pre-compound emission in the background direction. This discrepancy is illustrated more clearly in Figure 7 where comparison is made between measured[1] and calculated proton spectra at 124 degrees from 61.5-MeV protons incident on gold. This kind of discrepancy has been noted before and is somewhat ameloriated by the addition of refractive effects to the calculation.[23] More pre-compound emission at large angles will also occur if the incident nucleon strikes something heavier than a nucleon such as, for example, a pair of nucleons. The effect of such collisions has been investigated roughly and is illustrated by the dashed histogram in Figure 7.[1] This calculation was a rather unrealistic one in that it was assumed that all collisions were with nucleon pairs and the pairs were not transported through the cascade. Nevertheless, it is interesting to see the decisive effect brought about by collisions with objects heavier than nucleons.

F. Emission of Complex Particles: The inclusion of collisions with clusters of nucleons immediately brings us to the question of the possibility of the pre-compound emission of complex particles. It is well known, as exemplified by the data[1] presented in Figure 3 as well as recent investigations by Gadioli et al[26] and by Cline,[27] that such processes are of significance. Except for some pioneering work by Gradsztajn[28] in which alpha-particle clusters were explicitly included among the cascade particles in an approximate fashion, there has been no effort to investigate the effects of nucleon clustering on the cascade model. Not the least of the reasons for this oversight is the fact that it is not easy to see how to introduce this effect in other than an ad hoc fashion.

IV. MASTER EQUATION

A. Description of Model: Another approach to the solution of equation 1 for the W(E,Q,t) is by means of a master equation in which the state of the system is described by the occupation numbers of single-particle states and the time evolution of these occupation numbers is determined by two-body collisions.[19,20] To illustrate the general method, for a one component system a member of the set of coupled differential equations would be

$$\frac{d(n_i g_i)}{dt} = \sum_{j,k,l} W_{kl,ij}\, g_k n_k\, g_l n_l\, (1-n_i)(1-n_j)\, \frac{g_i g_j}{\Delta} - \sum_{j,k,l} W_{ij,kl}\, g_i n_i\, g_j n_j\, (1-n_k)(1-n_l)\, \frac{g_k g_l}{\Delta} - n_i g_i W_{i,i'} g_{i'} \qquad (3)$$

where n_i is the average occupation number of the states in energy interval $\underline{i}$ which is of width Δ, g_i is the number of states in energy interval $\underline{i}$, $\omega_{ij,kl}$ is the transition probability for a particle in one of the states $\underline{i}$ to collide with a particle in one of the states $\underline{j}$ to go to particles within the states $\underline{k}$ and $\underline{l}$, and $\omega_{ii'}$ is the transition probability for a particle in one of the states in the interval $\underline{i}$ within the nucleus to be emitted into one of the states in the interval $\underline{i}'$ outside of the nucleus. The condition on $\underline{i}$, $\underline{j}$, $\underline{k}$, $\underline{l}$ and $\underline{i}'$ are such that energy is conserved. The first two terms of equation 3 correspond, respectively, to the gain and loss of particles from interval $\underline{i}$ by two-body collisions; the third term accounts for the emission of particles from internal states in the interval $\underline{i}$.

A pictorial representation of the formalism is presented in Figure 8. As is indicated in Figure 8, the Fermi-gas model of the

nucleus was used although, as will be seen shortly, that is not necessary and shell-model states can just as well be employed. For the schematic process depicted in the figure, the incident particle occupies the 10th interval upon entering the nucleus which sets the boundary condition for zero time. The occupation of each interval then evolves according to equation 3 with the schematic results indicated by the succeeding two times illustrated in Figure 8. For the situation in Figure 8, it is only for $\underline{i} > 7$ that $\omega_{i,i'}=0$.

The internal transition probabilities, $\omega_{ij,kl}$ are determined from energy-dependent free-nucleon scattering cross sections under the assumption that all collisions are at right angles and that all energy-conserving two-particle final states are equally probable. Neutron and proton components are treated separately except, of course, neutron-proton collisions are included. For the single-component system, the transition probabilities are of the form

$$\omega_{ij,kl} = \frac{\sigma(\varepsilon_i+\varepsilon_j)\left[(2/M)(\varepsilon_i+\varepsilon_j)\right]^{1/2}}{V\sum_{mn} g_m g_n/\Delta} \qquad (4)$$

where $\sigma(\varepsilon_i+\varepsilon_j)$ is the free-nucleon scattering cross section for the relative velocity at the right-angle collision, V is the nuclear volume, M is the nucleon mass, and the summation in the denominator is over all energy-conserving and distinguishable final states.

The emission probability comes from detail-balance considerations and thus is of the form

$$\omega_{i,i'} = \frac{\sigma_{inv}\,(2\varepsilon'/M)^{1/2}}{g_i\,\Omega} \qquad (5)$$

where, as usual, σ_{inv} is the cross section for the inverse process, and Ω is an external normalization volume that cancels a similar term in $g_{i'}$. The solution to the pre-compound problem then,

requires the solution of the set of coupled equations of the type illustrated in equation 3. This is accomplished numerically on a computer using the Runga-Kutta-Gill method.[19]

Because of the third term in equation 3, the rate of change of occupation numbers will not vanish until the excitation energy is below that required for particle emission. Nevertheless, there is a time by which the emission of particles becomes the dominant effect and thus the distribution of occupation numbers becomes very close to that expected for a Fermi gas. This quasi-equilibrium distribution is the configuration that corresponds to the compound nucleus in the context of this model. The numerical methods do indeed converge on this result. This is illustrated in Figure 9 where the time evolution of a ^{238}U nucleus excited to 206 MeV is shown. In this calculation, the initial configuration for the two-component counterpart of equation 3 was taken from the final configuration of a single intra-nuclear cascade of the type described in Section III.[29] The distribution of occupation numbers after relaxation ($t=t_R$) corresponds to a Fermi gas at a temperature of about 2.6 MeV. The spectrum of neutrons emitted after relaxation has occurred has the expected shape and corresponds to a "temperature" of about 2.5 MeV for the usual "constant-temperature" approximation for the spectral shape.

It is worthy of mention in passing that even the initial configuration shown in Figure 9 bears some resemblance to that at equilibrium. This is, of course, as it should be since the intra-nuclear cascade calculation itself is mapping out the relaxation process.

B. Comparison With Experiment: It has already been pointed out that the solution of equations 3, 4, and 5 underestimates the amount of pre-compound decay. This is illustrated in Figure 6 where the result of the master-equation (the dotted curve designated as HMB) is compared with experimental data as well as other calculations. While the shape of the pre-compound spectrum is reproduced rather well, the magnitude is off by a factor of from two to three. A divergence of this magnitude had also been found for the

"hybrid" version of the exciton model.[10] Too little emission implies that the internal transition probabilities as represented by the first two terms of equation 3 are too large as compared to the emission of particles corresponding to the third term. This discrepancy is not surprising since, as was pointed out earlier[20] and demonstrated experimentally in Figure 3, the outer diffuse edge of the target nucleus is of decisive importance in these reactions whereas the internal transition probabilities that have been used correspond to the nuclear densities in the more central region of the nucleus. The effect of an ad hoc and arbitrary change in the internal-transition probabilities is illustrated in Figure 10. There it is seen that a reduction in the internal transition probabilities by a factor of four brings about considerably better agreement with the experimental results. Needless to say, an arbitrary reduction in this quantity by a factor of four is hardly acceptable. More will be said on this point in the following.

C. Effect of Shell-Model States: Of the three models discussed here, it is the master equation approach in which it is easiest to investigate the effects of introducing shell-model-like states in place of either the Fermi-gas or the uniform-spacing model. One aspect of the result of doing this is illustrated in Figure 11.[30] The proton occupation numbers are given at three different times in the course of the simulated reaction of 29 MeV protons with ^{54}Fe. As is expected simply from energy conservation, the presence of discrete bound states gives rise, at short times, to structure in the occupation numbers of the unbound states as seen in the solid curve in Figure 11 even though the latter were taken as part of a Fermi continuum. This structure will, of course, give rise to structure in the spectrum of emitted particles. There is, for example, a prominent peak at 76-MeV internally which results in a peak in the spectrum at 26 MeV corresponding to a transition in the target from the state at 45 MeV to that at 48. The dashed curve in Figure 11 shows that the effects of the discrete states are smoothed out in time and the internal configuration, and thus the spectrum of emitted particles, is essentially

the same as that for the corresponding Fermi-gas model for the nucleus.

No attempt was made in the calculation with discrete states that has just been described to keep track of angular-momentum conservation. Had that been done, and had the angular-momentum distribution of the unbound states been explicitly included, the internal-transition probabilities would have doubtless been reduced. This effect may well be part of the reason for the underestimate of the emission of pre-compound particles that has been discussed previously. On the other hand, it must be stated immediately that the concomitant presence of peaks in the emission spectrum at very short times cannot be taken seriously as a simulation of direct processes.

V. EXCITON MODEL

A. Description of the Model: The essence of the exciton model[6-18, 20, 25-27] is that it describes the state of an excited nucleus in terms of the number of excitons (excited particles + holes) that are present and assumes that two-body collisions occur which can change the exciton number by ±2. In addition, nucleons can be emitted which diminish the exciton number by 1. A crucial assumption is that all configurations consistent with the exciton number and the excitation energy are assumed to be equally likely. This assumption was tempered a bit by Williams[31] who estimated the average number of configurations at exciton number n+2 that are accessible by a two-body interaction from exciton number n.

The model is schematically represented in Figure 12 taken from Blann.[12] There it is seen that there are two classes of configuration for each exciton number: those with and those without particles in unbound states. The general scheme of the calculation is to estimate the probability that a particle is in an unbound state at each exciton number and that it escapes from the nucleus before the exciton number changes. If it is assumed, as need not be done,[9] that the density-of-states considerations cause transitions which lead from n to n+2 to be dominant for those values of n (small) important to pre-compound decay and if, for reasons of simplifying the discussion, a one component system is considered, then the spectrum of pre-compound particles may be written as

$$I(\varepsilon') = \sum_{m=m_0}^{m=\bar{m}} D_m \left[\frac{\rho_{m-1}(U)\, g(\varepsilon)}{\rho_m(E)}\right]\left[\frac{\lambda(\varepsilon'|E,m,\varepsilon)}{\lambda(\varepsilon'|E,m,\varepsilon)+\lambda(m+2|E,m,\varepsilon)}\right] \qquad (6)$$

where n_0 and $\bar{n}$ are the initial and equilibrium number of excitons, respectively; D_n is the probability that no particles have been emitted before the system arrives at exciton number n; $\rho_n(E)$ is the number of ways of distributing the excitation energy E among n excitons; $g(\varepsilon)$ is the density of single particle states at

energy ε above the bottom of the potential well inside the nucleus; $\lambda(\varepsilon'|E,n,\varepsilon)$ is the probability per unit time that a particle of kinetic energy ε' be emitted from a reacting system with excitation-energy E distributed over n excitons in such a manner that there is a particle in the level at energy ε within the nucleus that corresponds to the energy ε' outside the nuclear boundary; and $\lambda(n+2|E,n,\varepsilon)$ is the probability per unit time that there be a two-body collision in the reacting system just described that increases the exciton number from n to n+2.

The quantity in the first set of brackets is the expectation value of the number of particles in the level at ε under the assumption of equal a priori probability for all configurations of n excitons at excitation energy E and where $U = E-\varepsilon'-B$ (B is the binding energy of the emitted particle). It is to be noted that

$$\int_{\varepsilon_f}^{E} \frac{p_{n-1}(U)\, g(\varepsilon)}{p_n(E)}\, d\varepsilon = p \qquad (7)$$

where p is the number of excited particles and ε_f is the Fermi energy.

The quantity in the second set of brackets is the probability that the reacting system characterized by n, E, and ε emit the particle from the level at ε before a collision occurs that raises the exciton number to n+2.

It is primarily the assumption of equal a priori probabilities for all configurations of the distributions of particles and holes for the reacting system at excitation energy E with p excited particles and h holes that occasions the simple closed-form expression for the pre-compound spectrum for a one-component system as given in equation 6. The use of certain average quantities in place of the detailed bookkeeping on the time evolution of the reaction as employed in the previous two models also add to the simplification. Nevertheless, the calculation rapidly becomes more complex when an attempt is made to evaluate the various terms in equation 6.

While it is not appropriate here to go into detail on this point, it would be useful to sketch briefly in physical terms the problems that are encountered and the approximations that are made.

1) While there is no essential difficulty in evaluating $\rho_n(E)$ in terms of particle and hole numbers rather than just exciton number, there is difficulty in knowing this quantity when proper account is taken of both the Pauli exclusion principle and the finite limit on the depth of a hole in the Fermi sea.
2) While the distinction between neutrons and protons has been explicitly introduced,[27] it does not seem to have been done in a fashion that recognizes the distinction between the interactions of like and unlike nucleons.
3) The quantity that is the most difficult to estimate, is decisive to the amount as well as the spectral shape of pre-compound decay, and has generated the greatest volume of literature on the general subject, is the rate of internal transition, $\lambda(n+2|E,n,\varepsilon)$. These estimates include those that treat the internal transition rates by Fermi's Golden Rule number 2 with matrix elements independent of the configuration in question[31] and those that, similar to the previous two models, considers the two-body collisions classically as the equivalent collisions in free space. Within the latter context, there are two popular approaches:
   a) Possible collisions of all of the excited particles are to be considered
   b) Collisions only of the particle in the level at $\underline{\varepsilon}$ are to be considered.

   The second approach is, of course, considerably simpler and is the one of choice at the moment in what is known as the "Hybrid model".[10] Its use, though, raises serious questions about the consistency of the bookkeeping in that events may be counted more than once and, further, goes to the heart of the assumption of equal a priori probabilities for all configurations. This problem is currently under invesitgation by Gadioli et al.[32]

B. Edge Effects: Earlier formulations of the exciton model also underestimated the amount of pre-compound decay. This disability has been remedied in a recent reformulation of the calculation by Blann[13] which recognizes the importance of the longer mean-free-paths in the diffuse edge of the nucleus by lowering $\lambda(n+2|n,E,\varepsilon)$ correspondingly for the initial values of n. The salubrious effect of this modification is illustrated in Figure 6 by the impressive agreement between angle-integrated experimental and calculated results. The relevant calculated curves are labeled GDH (geomentry-dependent hybrid model); the two curves labeled "OPT" and "CON" correspond to using optical and continuum model calculations for the inverse cross section as in equation 5. Without the lowering of the internal transition rate because of edge effects, the exciton-model calculation would be similar to that calculated by the master equation which is designated as HMB in Figure 6.

C. Recent Advances: Before ending the sketch of the exciton model, a few words should be devoted to a recent development in the exciton model: an investigation of isospin conservation in pre-compound decay.

It has been known for some time that enhancement of compound-nucleus (p,p') reactions indicates the partial conservation of isotopic spin.[33] In a recent further investigation of this phenomenon, Kalbach-Cline et al[34] suggest that isospin conservation also plays a role in the pre-compound emission of protons in the reaction of protons with tin. The primary point is that the reactions proceed partly through two unmixed isospin states, $T_>=T+1/2$ and $T_<$ with $T=T-1/2$, where T is the isospin of the target nucleus, and that the emission of particles from these two states, both pre-compound and compound, can be quite different. In particular, it is expected that the probability of proton emission from the $T_>$ state is considerably enhanced over that from the $T_<$ state. This occurs formally within the exciton model in that the term $\rho_{n-1}(U)$ in equation (6) corresponds to the normal isospin state, T, of the residual nucleus while $\rho_n(E)$ corresponds to the $T_>$ of the reacting compound system. Because of the much greater level density of the

normal T-states than that for the $T_>$-states at the same excitation energy, the first bracket in equation 6 can have a value considerably greater than unity even though the residual excitation energy U is less than the original value E. While this will surely lead to substantial pre-compound emission, it is not in accord with the physical meaning of the quantity in the first bracket as expressed in equation 7. It appears that this disability is a fundamental one whose source probably lies partly in the effort to ascribe a state of definite isospin to a given exciton number or to a particular configuration of particles and holes; and, perhaps more importantly, the inaccessibility of many normal T-states of the residual nucleus within the constraints of the model immediately subsequent to the emission of a particle. The implications of this problem for emission from an equilibrated compound nucleus in the $T_>$ state also merit investigation.

Finally, it should be mentioned that there has been an interesting exploration by Kalbach-Cline[27] of the extension of the exciton model to the pre-equilibrium emission of complex particles.

VI. PRESENT SITUATION AND PROSPECTS

While the three models that have been discussed are all fundamentally the same in that they are classical in the sense of equation 1 and include only two-body interactions, they differ markedly in detail and thus in their strengths and weaknesses.

It is only the intranuclear cascade calculations that naturally include the geometrical details of the problem and thus account for the effects of the diffuse edge as well as yield the angular distribution of the emitted particles. It reproduces angle-integrated spectra quite well when refractive effects are arbitrarily ignored but seem to require refraction to reproduce spectral shapes in the forward direction. This dilemma has yet to be reconciled and its implications discerned.

The major shortcoming of the cascade calculations other than the complexity of the requisite computer code, is that it ignores all holes once they have been created as well as interactions of particles below the Fermi level with each other. It appears doubtful, though, that these interactions are of significance to the main results of the calculation. The arbitrary energy cut-off below which cascade particles are no longer considered (see the initial neutron configuration in Figure 9) is chosen for convenience and is not an essential weakness of the formalism.

The other side of the coin, of course, is that neither the exciton nor the master-equation formalism naturally includes the geometrical aspects of the problem including the role of the diffuse edge. This obviates the possibility of calculating angular distributions and appears to be the source of the underestimation of pre-equilibrium decay. This latter difficulty has been investigated in what is called the "geometry-dependent-hybrid" model (GDH) by Blann[13] who ameliorates the problem by diminishing the $\lambda(n+2|n,\varepsilon,E)$ in equation 6 for the initial values of $\underline{n}$ in recognition of the fact that least the first interaction has a high probability of occurring in the diffuse edge of the nucleus. As shown in Figure 6, this refinement can lead to rather good agreement with experimental results. Figure 10 illustrates a similar

effect when the corresponding refinement is introduced in a less sophisticated and more ad hoc manner in the master equation: reduction of the internal transition probabilities in equation 3. However, angular distributions are still not calculable and, as can be seen from Figures 5 and 6, comparisons between calculated and experimental spectra after integration over angle can be quite misleading as an indication of the validity of the model.

The introduction of shell-model states into the master equation as described in section IVc would also diminish the internal-transition probabilities if angular-momentum conservation were explicitly included. That is to say, the $\omega_{ij,kl}$ in equation 3 could only decrease if angular momentum as well as energy conservation were imposed on the states involved.

Details aside, the main differences between the exciton as compared to the other two formalisms is that the exciton model assumes as known the quantity that the other two models spend most of the time calculating: the distribution among energy states of the excited particles and holes. In the exciton model all accessible configurations are taken to be equally likely and thus it is essentially an equilibrium model with the equilibrium steadily expanding to include more of the nucleons in the reacting system. Further, the rate of expansion (the internal transition probabilities) is taken as some average quantity in the exciton model while in the other two formalisms this rate is explicitly and laboriously calculated in terms of the assumed two-body interaction. While it is not at all clear that this equilibrium-like assumption is in general viable, it is probably not bad for the distribution of excited particles after the first collision since the two-body interactions should largely be in relative s-states. It is also important that the finite depth of the Fermi sea and the Pauli expulsion principle be included in the counting of configurations. The distribution of particles in more complex configurations, on the other hand, depends on the relative probabilities of the possible collision partners and thus depends on the details of the two-body interactions as a function of relative energy and particle identity. The main consequence of this difficulty is probably

not because of an error in the distribution of holes, but rather in the relative numbers of neutrons and protons among the excited (and emitted) particles. The approximations for the calculation of internal transition rates within the exciton model have been described toward the close of Section V A. They grow ever more complex and it is not clear if any of the various averaging approximations will be finally viable. The great influence of the exciton formalism has been in its simplicity; it remains to be seen if one can avoid its increasing refinement forcing it also to become a computer-bound calculation.

The assumption of equilibrium among the holes and excited particles allows for the inclusion of complex particles in the entrance and/or exit channels within the context of the exciton model. All that is necessary is to alter the appropriate exciton number and to keep track of the identity of the excited particles.[9,27] It would be considerably more difficult to introduce clusters of nucleons to either the master equation or the cascade model. Considerable success has been achieved, for example, in reproducing the high-energy tails on (α,n) excitation functions in terms of pre-compound neutron emission.[8,11,16,35] In this connection, excitation functions for an (α,n) and a (p,n) reaction that proceed through the same reacting system is presented in Figure 13.[36] It is interesting to note the congruence, particularly at high energies, of the excitation functions as a function of the excitation energy which implies a similar congruence of the pre-compound neutron spectra. This result is not in agreement with present treatments of pre-compound emission induced by alpha particles as compared to protons. It would appear to be useful if more such experimental investigations could be carried out as a help to the formulation of pre-compound processes induced by complex particles.

Finally, what is needed most of all is a persuavsive demonstration either that these classical approximations to the problem can be made fundamentally acceptable or that they should be abandoned forthwith.

Figures

1) Spectra from the (p,xp) reaction for 62 MeV proton on ^{54}Fe at 37 degrees, and on ^{54}Fe and ^{60}Ni at 40 degrees. The broad dashed bin near 10 MeV in the otherwise solid line represents the average cross section for $^{60}Ni(p,xp)$ in the region where cross sections for this run were affected by a temporary "dead" layer in the detection system. A gap is shown in the ^{54}Fe (p,xp) curve from 6-15 MeV; beyond this energy the continuum cross sections are the same within uncertainty. Figure and caption taken from reference 1.

2) Schematic diagram of intranuclear cascade generated by a proton with impact parameter b. The solid circles indicate positions of collisions; the open circles indicate collisions that were forbidden by the Pauli exclusion principle. The short arrows ending within the nucleus indicate "captured" nucleons that contribute to the over-all excitation.

3) Dependence of pre-compound particle cross section on mass number of target. The ordinate shows the measured cross section divided by $A^{1/3}$ while the abscissa is plotted in units of $A^{1/3}$ for convenience. Figure taken from reference 1.

4) ^{27}Al (p,xp) spectra for incident protons of 61.9 MeV. The measured spectra are shown in bins for energies below the obvious discrete peaks. The intranuclear-cascade plus evaporation model calculation of Bertini is shown as a histogram with steps broader than those used for the data. The dashed histogram at 15 and 45 degrees is the Brookhaven-Columbia calculation which includes the effects enumerated in the text but does not include an evaporation contribution. Note that the high-energy peaks at small angles are often off scale. Figure taken from reference 1.

5) $^{209}Bi(p,xp)$ spectra. See Figure 4 caption. Figure taken from reference 1.

6) Comparisons of experimental[1] and calculated $^{209}Bi(p,xp)$ spectra at incident energies of 39 and 62 MeV. The various calculations are as follows: the curve designated "Cascade BNL" is described in sections III C and D; "Cascade ORNL" is described in section III B; "HMB" is described in section IV A; "GDH" is described in section V B. Figure taken from reference 25.

7) $^{197}Au(p,xp)$ spectrum 124 degrees with 61.5-MeV incident protons. The experimental data are shown as a histogram with 1-MeV bins, the standard Monte Carlo calculation as a wider solid histogram, and the modified nucleon "pair model" as a dashed histogram. The calculations did not include evaporation. The calculations did not include transport, "decay", or escape of the struck nucleon pair. Figure taken from reference 1.

8) Schematic representation of the consequences of equation 3 for 3 different times. The fraction of each energy bin that is shaded indicates the average occupation number. Figure taken from reference 25.

9) Proton and Neutron occupation numbers versus energy for an initial configuration (t=0) resulting from an intra-nuclear cascade generated by a 200-MeV proton on ^{238}U and after relaxation (t=tR). Figure is taken from reference 20 where more details are given.

10) Calculated and experimental[1] energy spectra for protons emitted in reactions between ^{54}Fe and 62-MeV protons. The dash-dot curve is calculated from the master equation with a nuclear density corresponding to a nuclear-radius parameter of 1.5 Fermis. The dashed curve is the same calculation with the internal-transition probabilities reduced by a factor of 4.

11) Occupation numbers of approximate proton single-particle states in the reaction of 29-MeV protons with ^{54}Fe. The energies of the single-particle states are designated by numbers and arrows;

11) the numbers in parentheses are the corresponding degeneracies. The vertical line at 50 MeV represents the top of the potential-energy well. Levels above 50 MeV are taken to be those of a Fermi gas.

12) Pictorial representations of the ideas inherent in the exciton model. The series of two-body interactions leading toward an equilibrium distribution is illustrated, as well as the possibility of the configuration at each exciton number of having one or more particles in unbound states.

13) Cross section versus excitation energy for the designated reactions. It is accidental that in these reacting systems the binding energies and Coulomb barrier are such that the total reaction cross sections are very similar at bombarding energies corresponding to the same excitation for the ^{143}Pr reacting system.

References

*Work supported by the United States Atomic Energy Commission

1) F.E. Bertrand and R.W.Peele; to be published in Phys. Rev.

2) Robert Serber, Phys. Rev. 72, 1114(1947).

3) M. Goldberger, Phys. Rev. 74, 1269(1948).

4) N. Metropolis, R. Bivins, M. Storm, A. Turkevich, J. Miller and G. Friedlander, Phy. Rev. 110, 185(1958).

5) V.S. Barashenkov, H.W. Bertini, K. Chen, G. Friedlander, G.D. Harp, A.S. Iljinov, J.M. Miller, and V.D. Toneev, Nucl. Phys. A187, 531(1972).

6) J. Griffin, Phys. Rev. Letters, 17, 478(1966).

7) M. Blann, Phys. Rev. Letters, 21, 1357(1968).

8) M. Blann and F.M. Lanzafame, Nucl. Phys. A142, 559(1970).

9) C.K. Cline and M. Blann, Nucl. Phys. A172, 225(1971).

10) M. Blann, Phys. Rev. Lett. 27. 337(1971).

11) M. Blann and A. Mignerey, Nucl. Phys. A186, 245(1972).

12) W.W. Bowman and M. Blann, Nucl. Phys. A131, 513(1969).

13) M. Blann, Phys. Rev. Lett. 28, 757(1972).

14) C. Birattari, E. Gadioli, A.M. Grassi-Strini, G. Tagliaferri, and L. Zetta, Nucl. Phys. A166, 605(1971).

15) E. Gadioli, Nuovo Cim. Lett. 3, 515(1972).

16) L. Milazzo-Colli and M.G. Braga-Marcazzan, Phys. Lett. 36B, 447(1971) and 38B, 155(1972).

17) P. Guazzoni, I. Iori, S. Micheletti, N. Molko, M. Pignanelli, and G. Semenescari, Phys. Rev. C4, 1092(1971).

18) E. Gadioli, I. Iori, N. Molko, and L. Zetta, Phys. Rev. C4, 1412(1971).

19) G.D. Harp, J.M. Miller, and B.J. Berne, Phys. Rev. 165, 1166 (1968).

20) G.D. Harp and J.M. Miller, Phys. Rev. C3, 1847(1971).

21) H.W. Bertini; Phys. Rev. 131 1801(1963), 138, AB2(1965), 188, 1711(1969).

22) K. Chen, Z. Fraenkel, G. Friedlander, J.R. Grover, J.M. Miller, and Y. Shimamoto, Phys. Rev. 166, 949(1968).

23) K. Chen, G. Friedlander, and J.M. Miller, Phys. Rev. 176, 1208 (1968).

24) K. Chen, G. Friedlander, G.D. Harp and J.M. Miller Phys. Rev. C4, 2234(1971).

25) Marshall Blann, Nuclear Equilibration Models for Nuclear Reactions at Moderate Excitations, U.S. Atomic Energy Commission Report #COO-3944-4.

26) E. Gadioli, I. Iori, N. Molko, and L. Zetta, Nuovo. Cim. Lett. 3, 677(1972).

27) C.K. Cline, Nucl. Phys. A193, 417(1972).

28) E. Gradsztajn, Phys. Rev. Lett. 13, 240(1964).

29) See reference 20 for a more detailed discussion of the initial configuration.

30) Personal communication from G.D. Harp.

31) F.C. Williams, Jr, Phys. Lett. 31B, 184(1970) and Nucl. Phys. A166, 231(1971).

32) E. Gadioli, E. Gadioli-Erba, and P.G. Sona, private communication. To be published in Nucl. Phys.

33) M.J. Fluss, J.M. Miller, J.M. D'Auria, N. Dudey, B.M. Foreman, Jr., L. Kowalski, and R.C. Reedy, Phys. Rev. 187, 1449(1969); C.C. Lu, J.R. Huizenga, C.J. Stephen, and A.J. Gorski, Nucl. Phys. A164, 225(1971); S.M. Grimes, J.D. Anderson, A.K. Kerman, and C. Wong, Phys. Rev. C5, 85(1972).

34) C. Kalbach-Cline, J.R. Huizenga, and H.K.Vonach, Preprint UR-NSRL-68.

35) R. Demeyer, R. Chery, A. Chevarier, J. Tousset, and Tran Minh-Duc, Journ de Phys. 31, 225(1970); and R. Demeyer, R. Chery, N. Chevarier, A. Chevarier, J. Tousset and Tran Minh-Duc, Journ. de Phys. 31, 847(1970).

36) E.V. Verdieck and J.M. Miller, Phys. Rev. 153, 1253(1967).

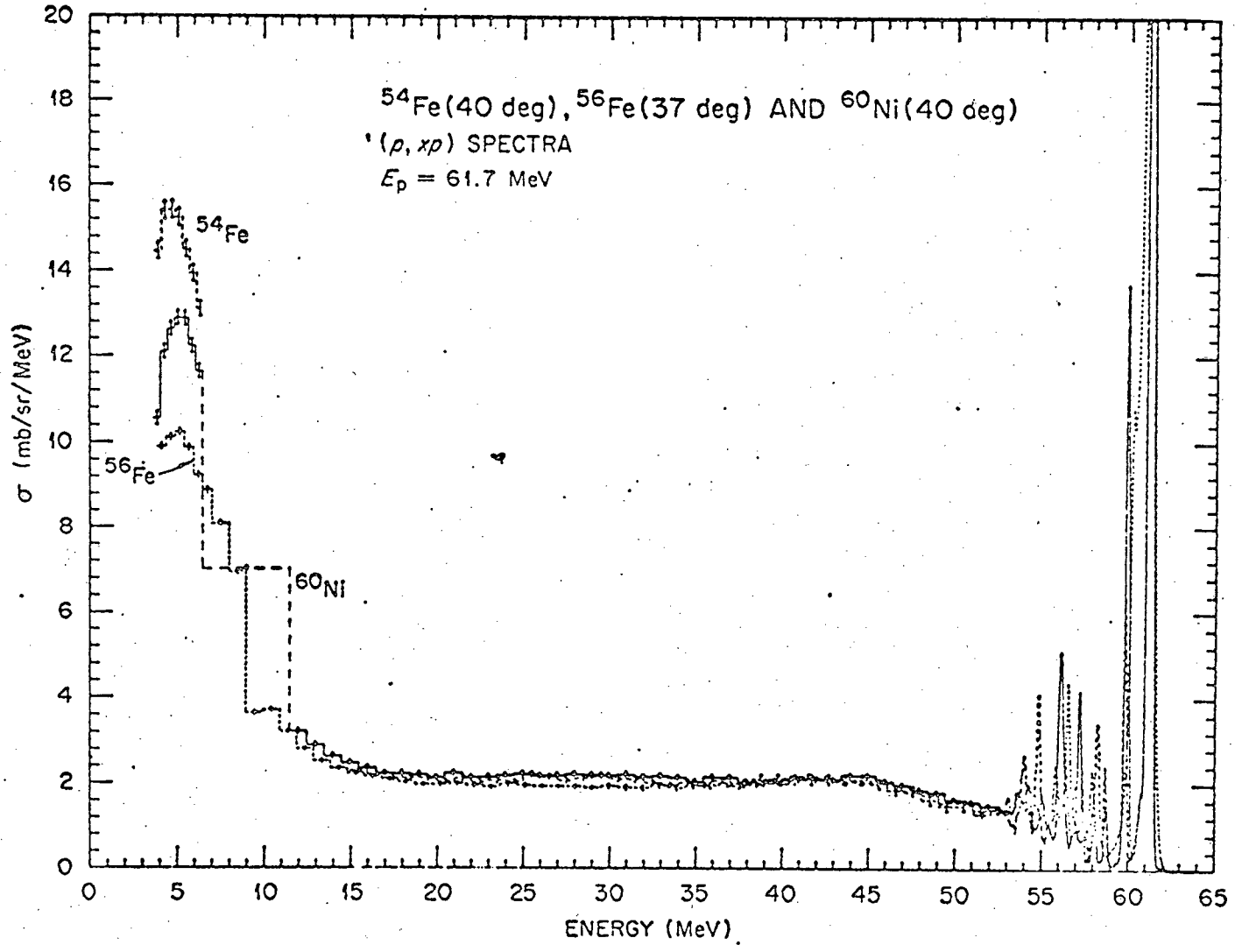
^{54}Fe(40 deg), ^{56}Fe(37 deg) AND ^{60}Ni(40 deg)
^{1}(p, xp) SPECTRA
E_p = 61.7 MeV
^{54}Fe
^{56}Fe
^{60}Ni
σ (mb/sr/MeV)
ENERGY (MeV)
0
2
4
6
8
10
12
14
16
18
20
0
5
10
15
20
25
30
35
40
45
50
55
60
65

Figure 1

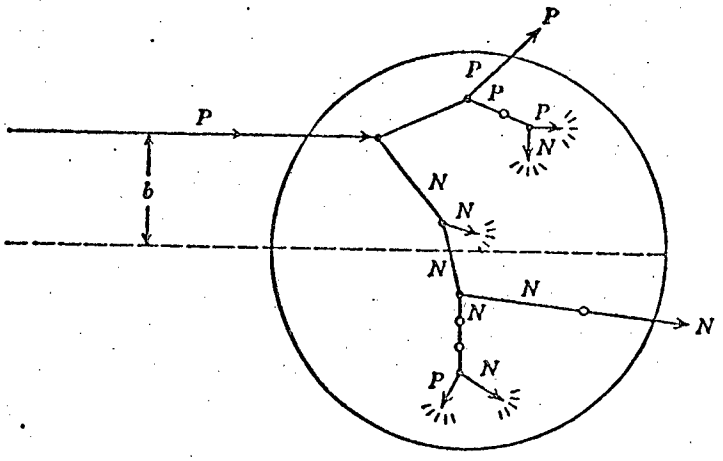

Figure 2

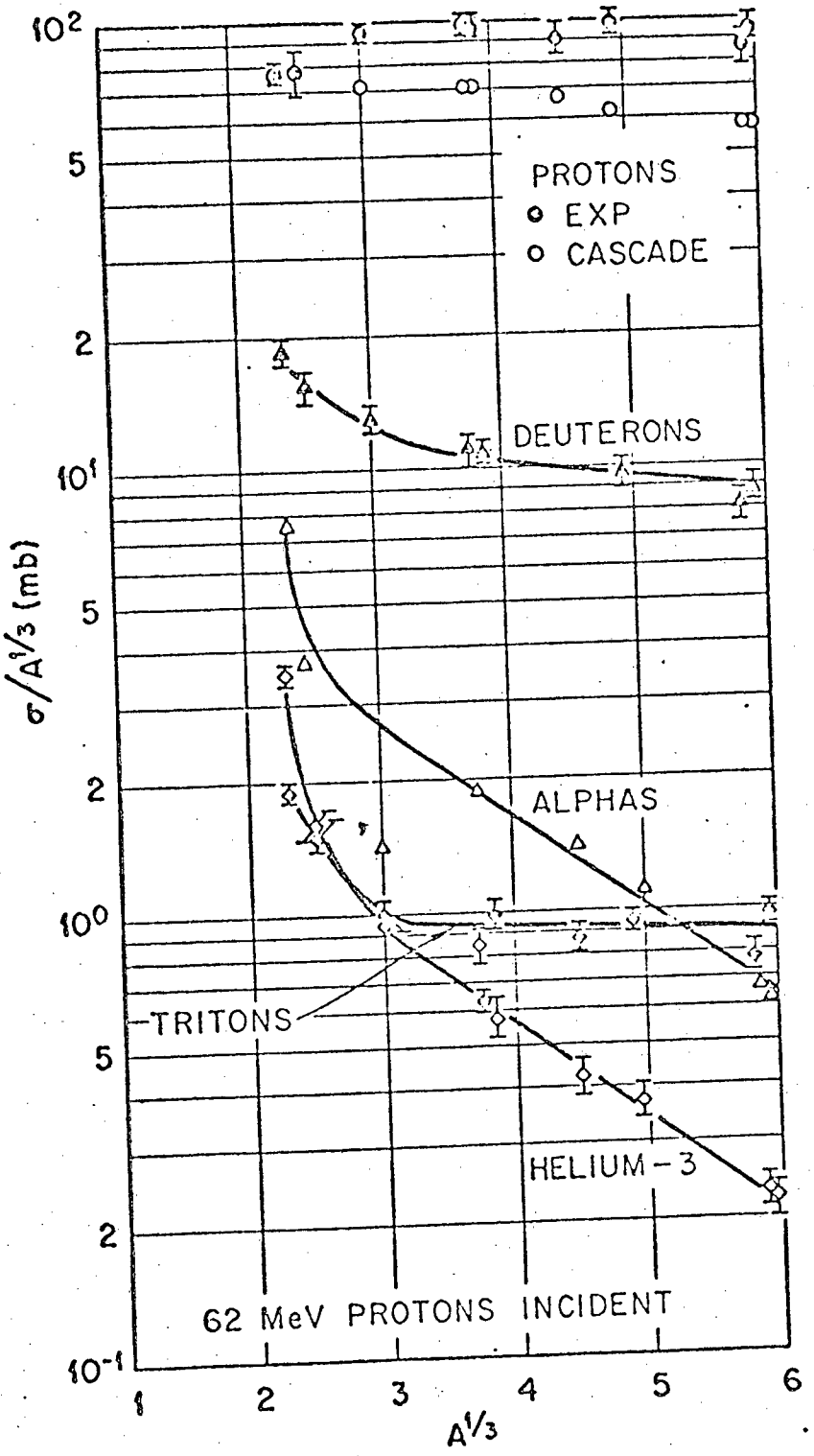
PROTONS
EXP
CASCADE
DEUTERONS
ALPHAS
TRITONS
HELIUM-3
62 MeV PROTONS INCIDENT
σ/A^1/3 (mb)
A^1/3
10^2
5
2
10^1
5
2
10^0
5
2
10^-1
1
2
3
4
5
6

Figure 3

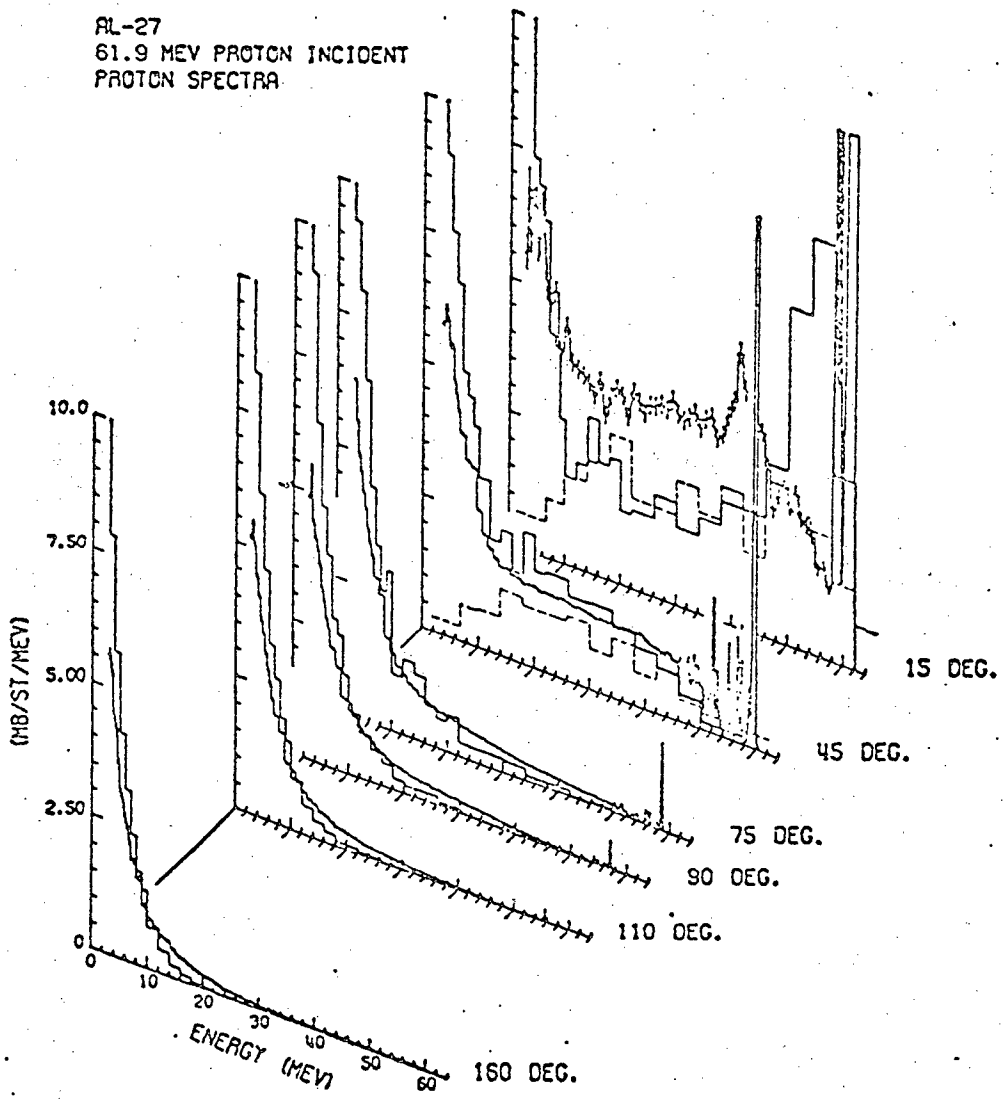
AL-27
61.9 MEV PROTON INCIDENT
PROTON SPECTRA
10.0
7.50
5.00
2.50
0
(MB/ST/MEV)
0
10
20
30
40
50
60
ENERGY (MEV)
15 DEG.
45 DEG.
75 DEG.
90 DEG.
110 DEG.
160 DEG.

Fig. 4

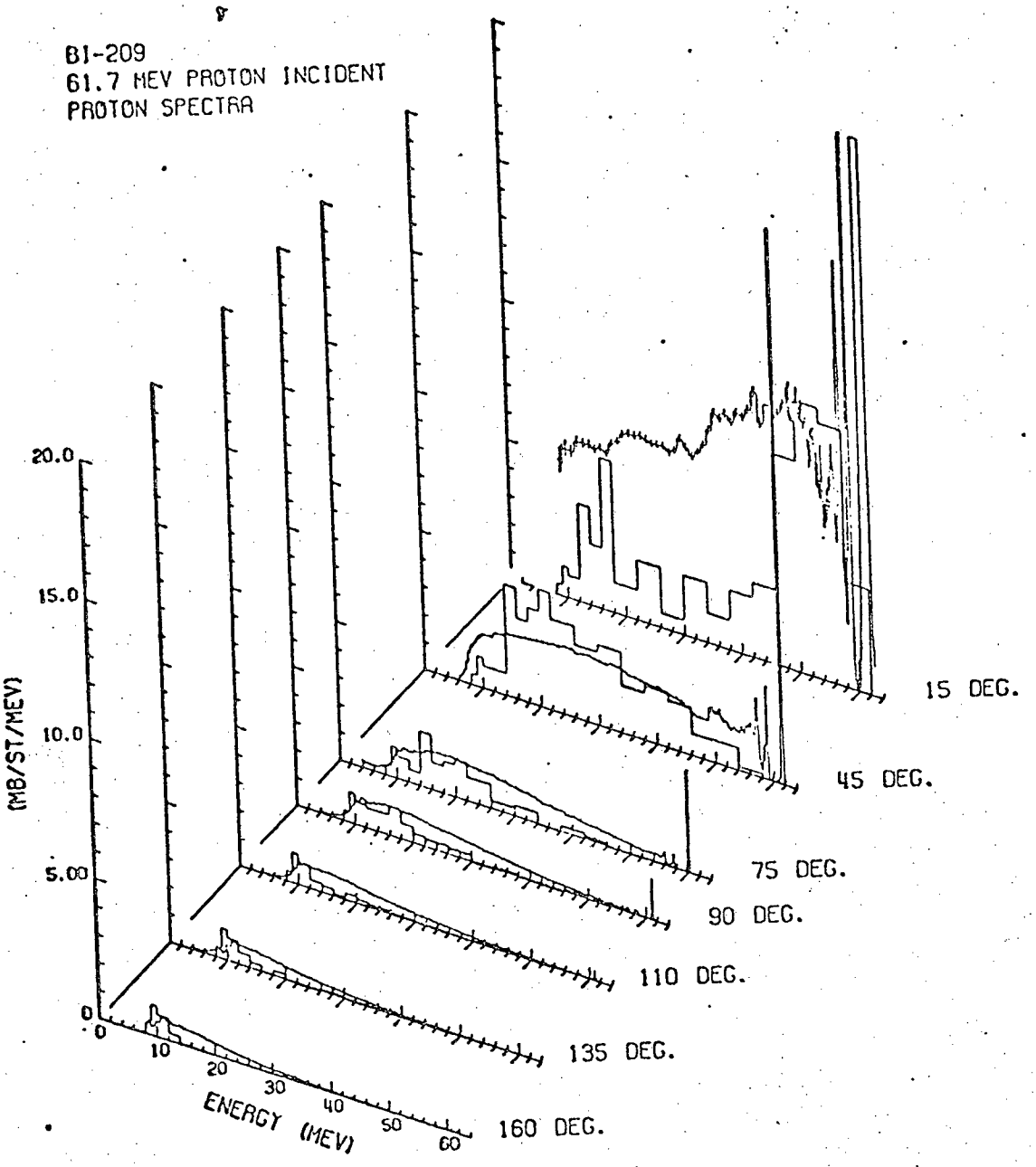
BI-209
61.7 MEV PROTON INCIDENT
PROTON SPECTRA
20.0
15.0
10.0
5.00
0
(MB/ST/MEV)
0
10
20
30
40
50
60
ENERGY (MEV)
15 DEG.
45 DEG.
75 DEG.
90 DEG.
110 DEG.
135 DEG.
160 DEG.

Figure 5

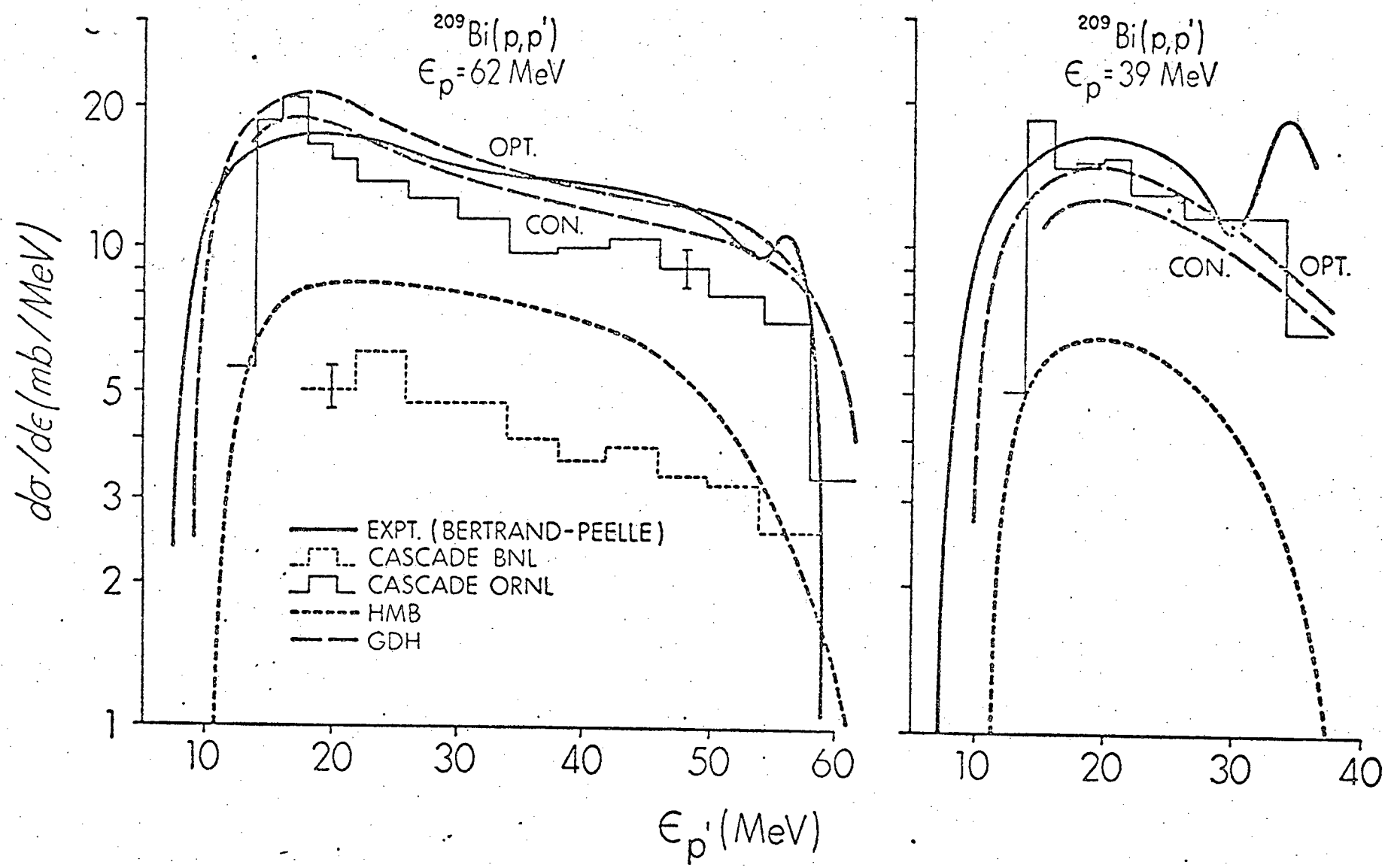
^{209}Bi(p,p')
ϵ_p=62 MeV
OPT.
CON.
EXPT. (BERTRAND-PEELLE)
CASCADE BNL
CASCADE ORNL
HMB
GDH
$d\sigma/d\epsilon$ (mb/MeV)
$\epsilon_{p'}$ (MeV)
^{209}Bi(p,p')
ϵ_p=39 MeV
CON.
OPT.

Figure 6

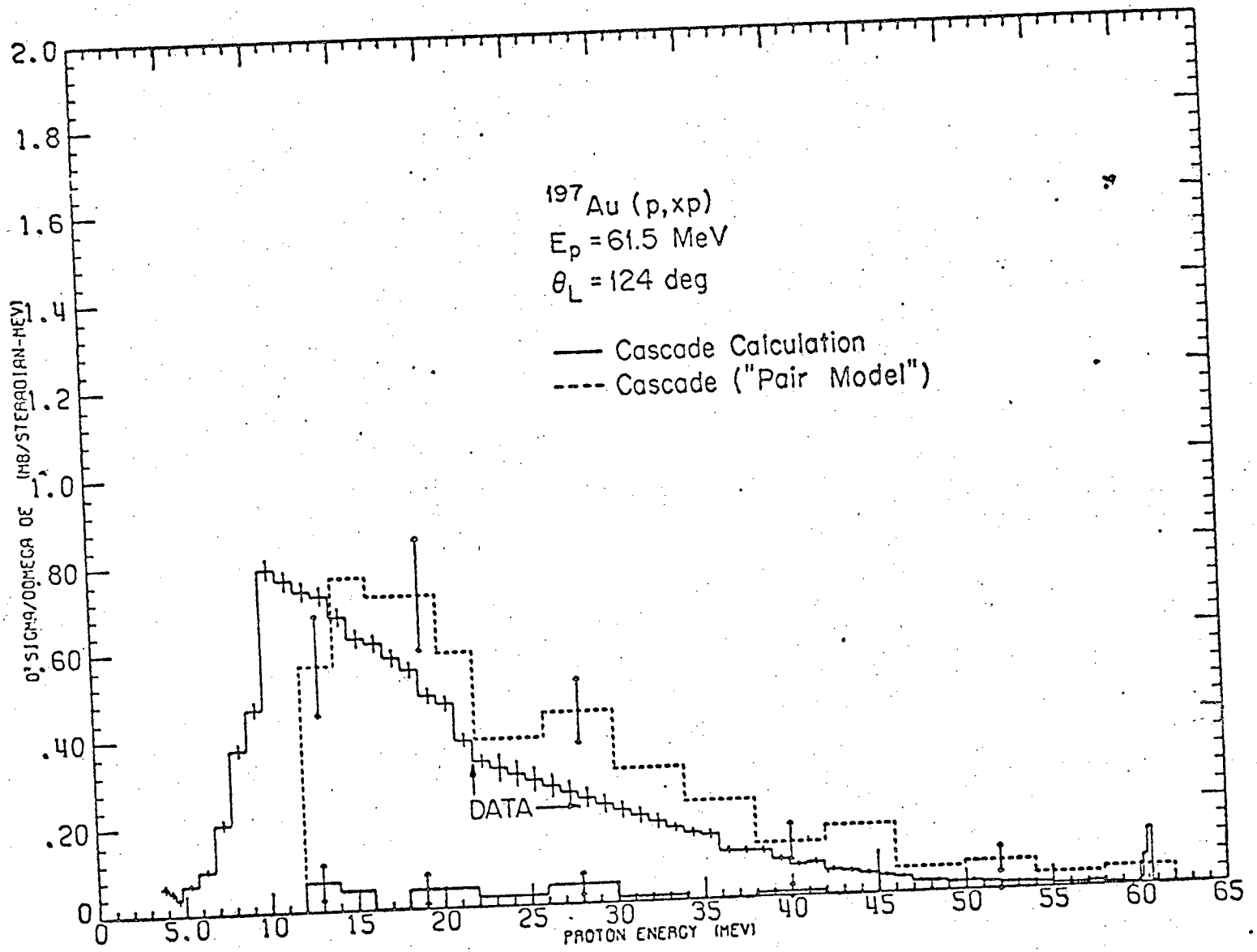
^{197}Au (p,xp)
E_p = 61.5 MeV
θ_L = 124 deg
Cascade Calculation
Cascade ("Pair Model")
DATA
d²SIGMA/dOMEGA dE (MB/STERADIAN-MEV)
PROTON ENERGY (MEV)
0
.20
.40
.60
.80
1.0
1.2
1.4
1.6
1.8
2.0
5.0
10
15
20
25
30
35
40
45
50
55
60
65

Figure 7

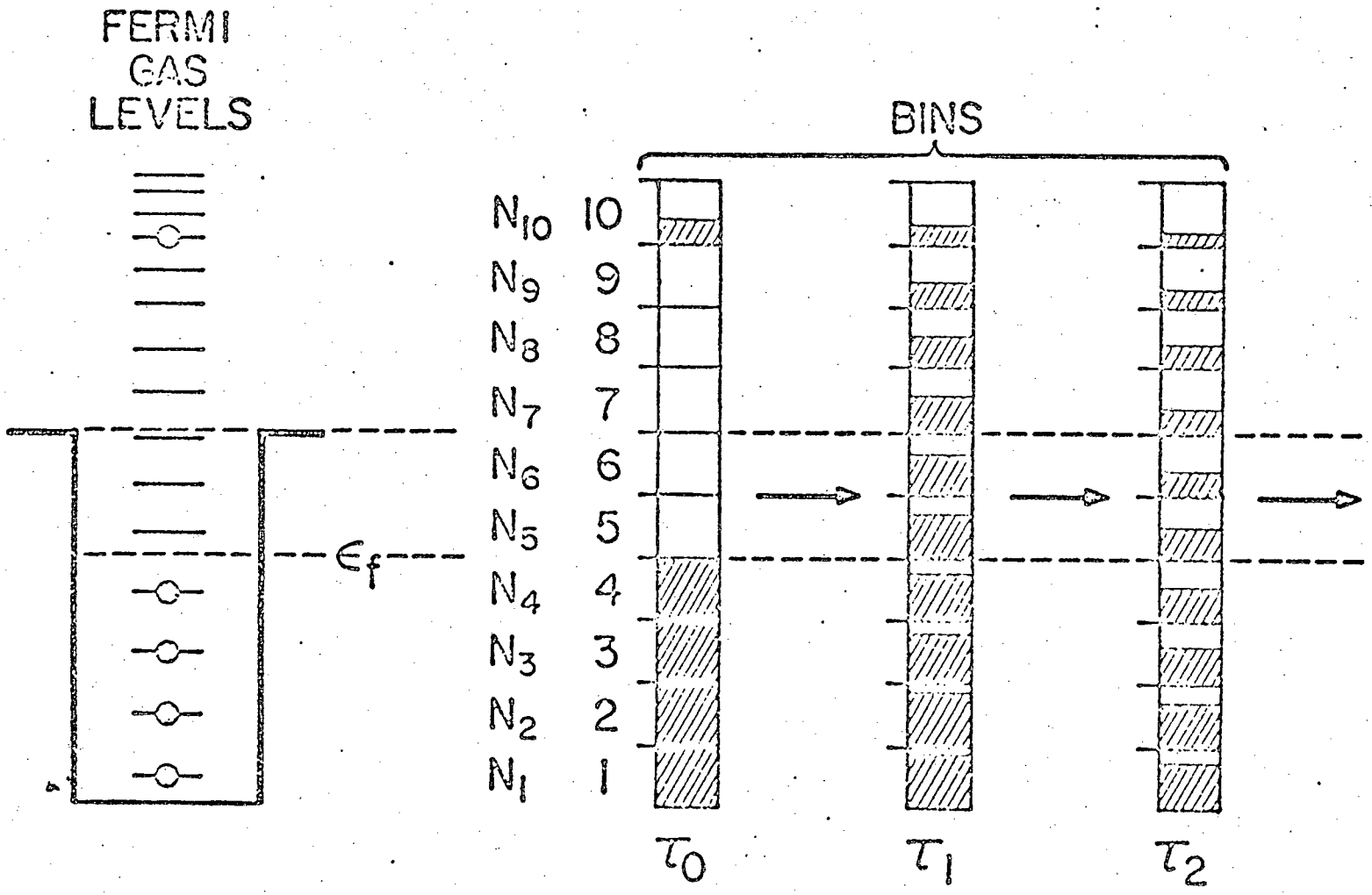
FERMI
GAS
LEVELS
BINS
N_{10} 10
N_9 9
N_8 8
N_7 7
N_6 6
N_5 5
N_4 4
N_3 3
N_2 2
N_1 1
ϵ_f
τ_0
τ_1
τ_2

Figure 8

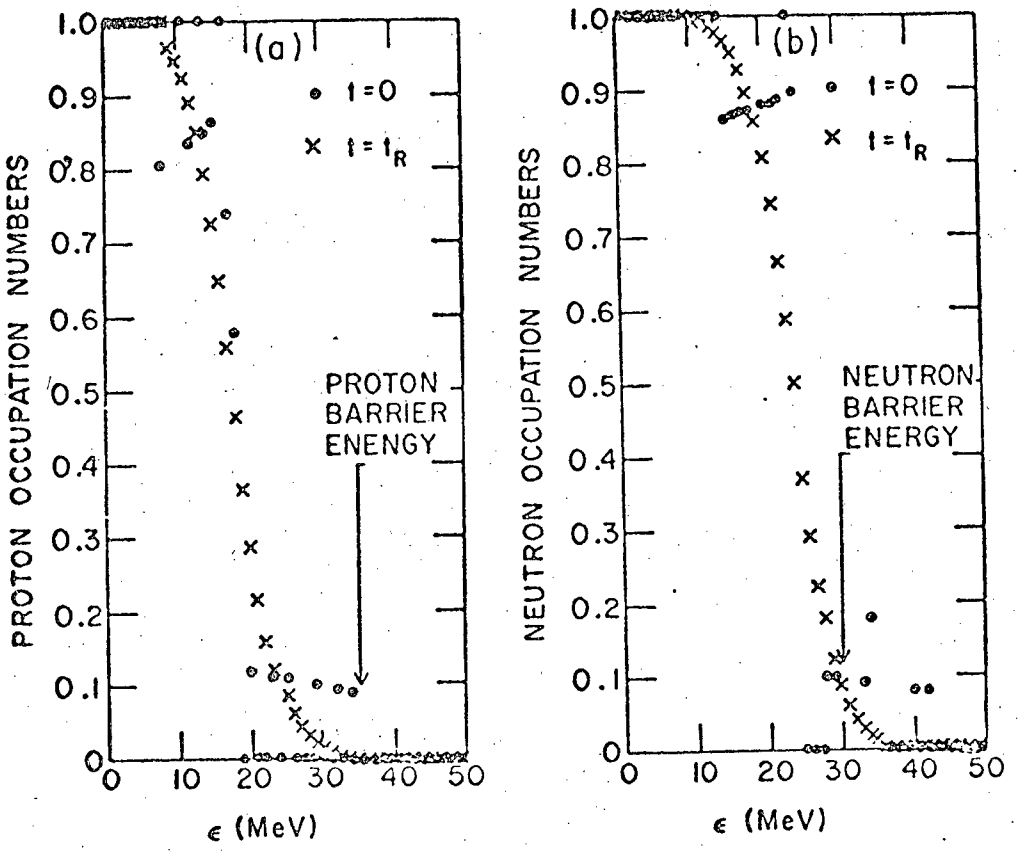
(a)
t=0
t = t_R
PROTON BARRIER ENENGY
PROTON OCCUPATION NUMBERS
ϵ (MeV)
(b)
t=0
t = t_R
NEUTRON BARRIER ENERGY
NEUTRON OCCUPATION NUMBERS
ϵ (MeV)

Figure 9

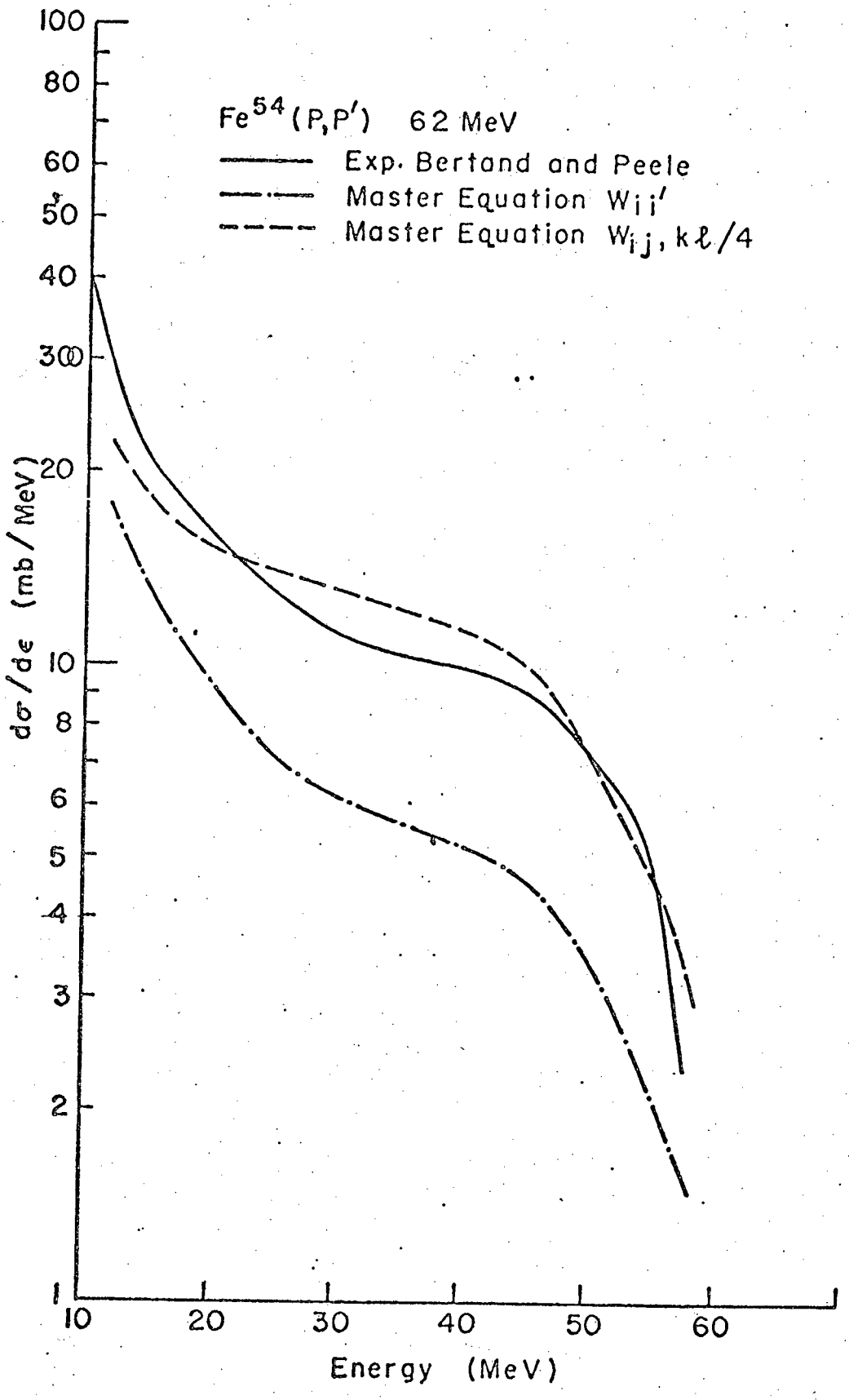
$Fe^{54}(P,P')$ 62 MeV
Exp. Bertand and Peele
Master Equation $W_{ij'}$
Master Equation $W_{ij,k\ell}/4$
dσ/dε (mb/MeV)
100
80
60
50
40
30
20
10
8
6
5
4
3
2
1
10
20
30
40
50
60
Energy (MeV)

Figure 10

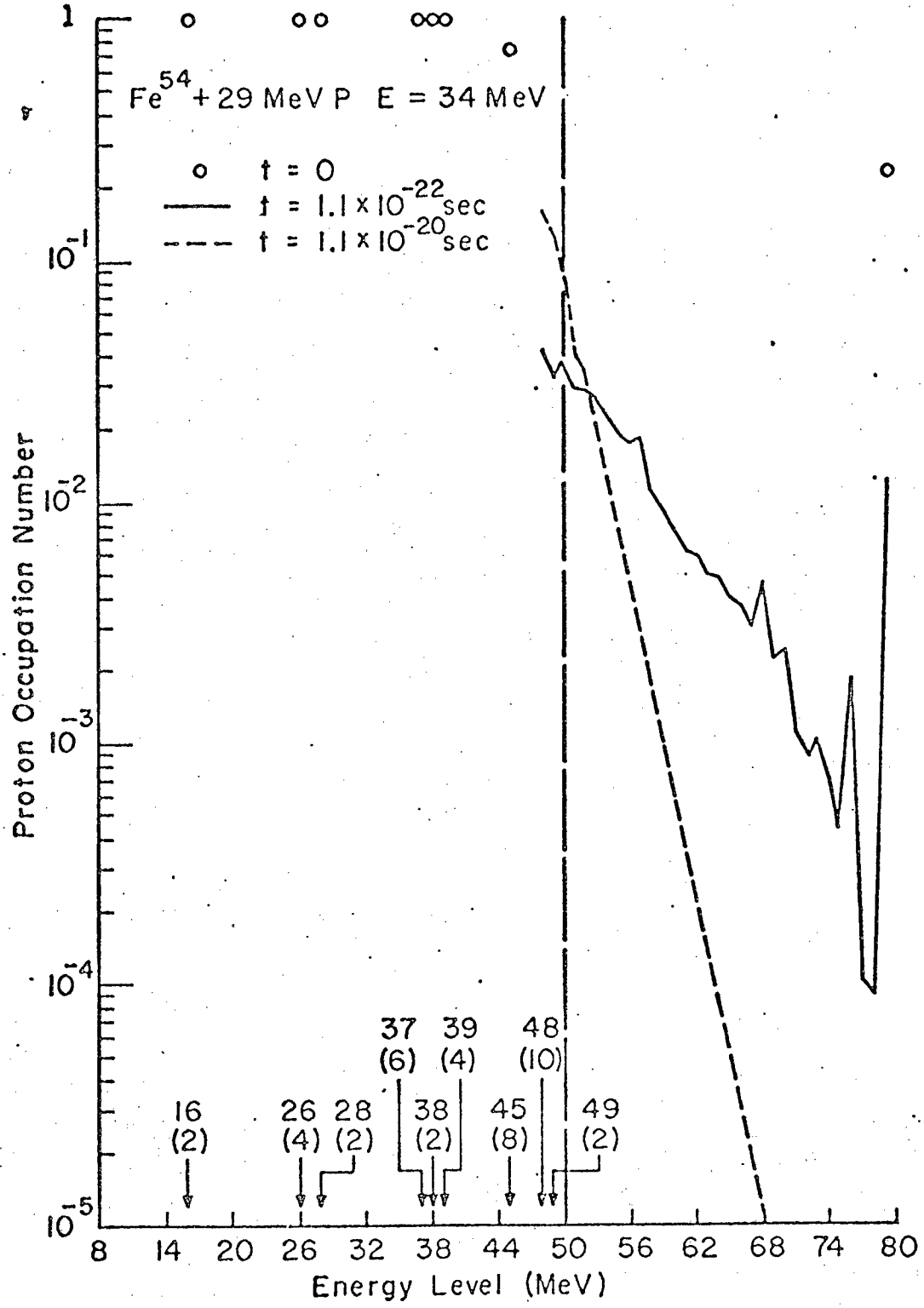
1
10^{-1}
10^{-2}
10^{-3}
10^{-4}
10^{-5}
Proton Occupation Number
Fe^{54} + 29 MeV P E = 34 MeV
t = 0
t = 1.1×10^{-22} sec
t = 1.1×10^{-20} sec
16 (2)
26 (4)
28 (2)
37 (6)
38 (2)
39 (4)
45 (8)
48 (10)
49 (2)
8 14 20 26 32 38 44 50 56 62 68 74 80
Energy Level (MeV)

Figure 11

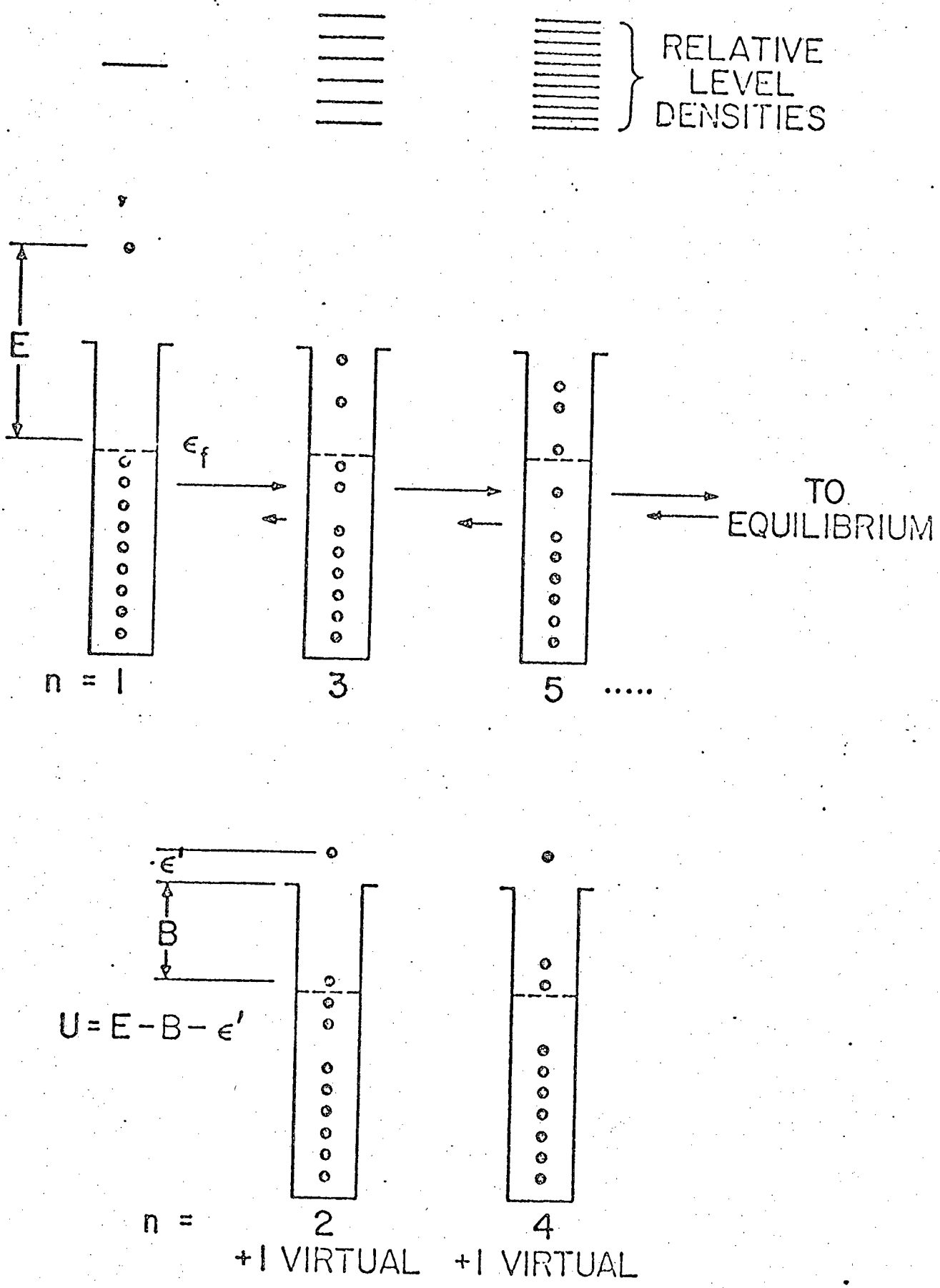
RELATIVE
LEVEL
DENSITIES
E
ϵ_f
TO
EQUILIBRIUM
n = 1
3
5 .....
ϵ'
B
U = E - B - ϵ'
n =
2
4
+1 VIRTUAL
+1 VIRTUAL

Figure 12

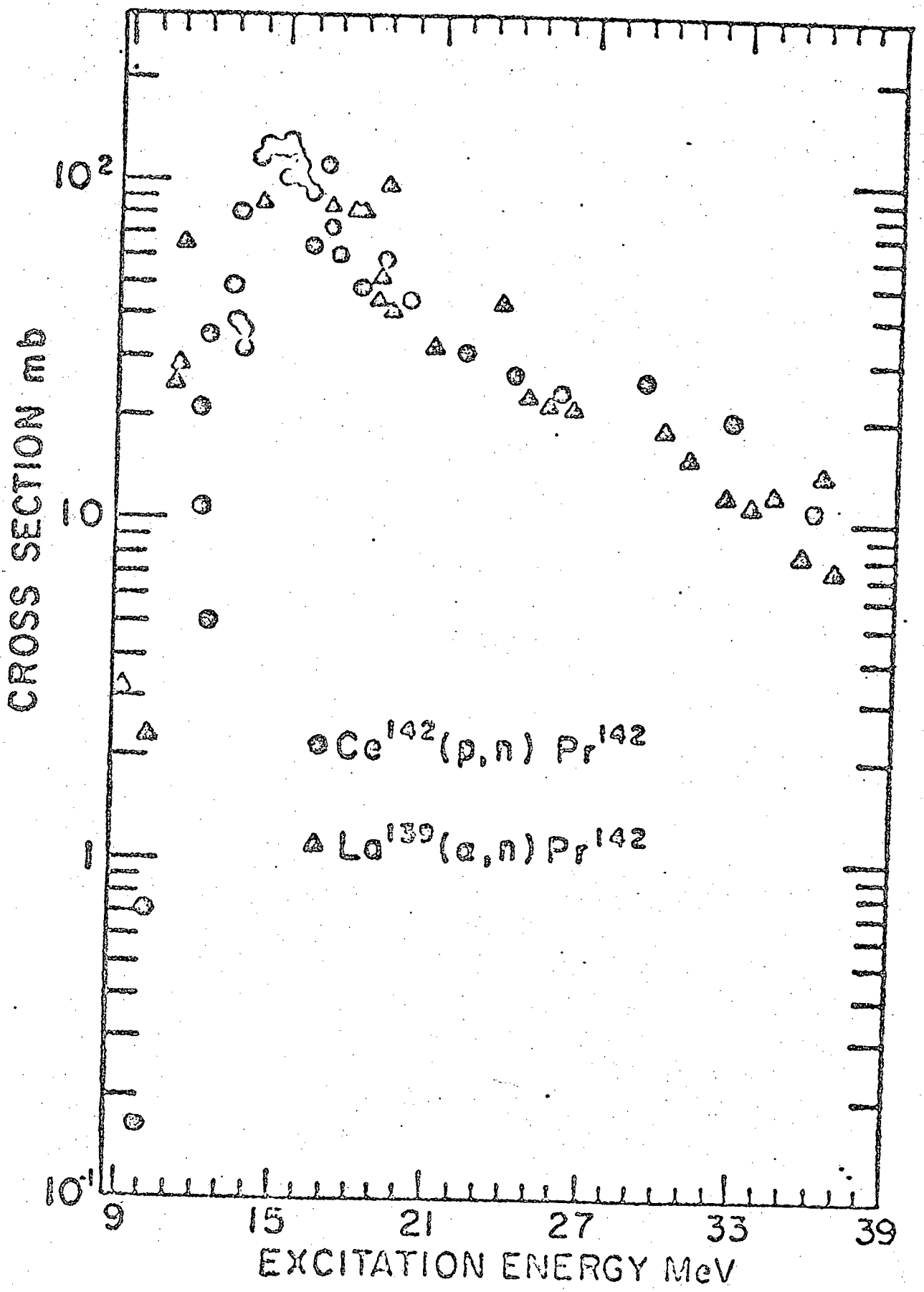
CROSS SECTION mb
10^2
10
1
10^{-1}
9
15
21
27
33
39
EXCITATION ENERGY MeV
$Ce^{142}(p,n)\ Pr^{142}$
$La^{139}(\alpha,n)\ Pr^{142}$